Published in final edited form as:
Dev Biol. 2009 June 1; 330(1): 142–152. doi:10.1016/j.ydbio.2009.03.020.

A Missense Mutation in the *Capza3* Gene and Disruption of F-actin Organization in Spermatids of *repro32* Infertile Male Mice

Christopher B. Geyer[1], **Amy L. Inselman**[1], **Jeffrey A. Sunman**[2], **Sheila Bornstein**[3], **Mary Ann Handel**[3], and **Edward M. Eddy**[1,*]

1 *Laboratories of Reproductive and Developmental Toxicology, National Institutes of Health, Research Triangle Park, NC 27709 USA*

2 *Molecular Carcinogenesis, National Institute of Environmental Health Sciences, National Institutes of Health, Research Triangle Park, NC 27709 USA*

3 *The Jackson Laboratory, Bar Harbor, ME 04609, USA*

Abstract

Males homozygous for the *repro32* ENU-induced mutation produced by the Reproductive Genomics program at The Jackson Laboratory are infertile, have low epididymal sperm concentrations, and produce sperm with abnormally shaped heads and poor motility. The purpose of the present study was to identify the mutated gene in *repro32* mice and to define the structural and functional changes causing infertility and the aberrant sperm phenotype. In *repro32/repro32* mice, we discovered a failure to shed excess cytoplasm and disorganization of the middle piece of the flagellum at spermiation, resulting in the outer dense fibers being wrapped around the sperm head within a bag of cytoplasm. Using a candidate-gene approach, a mutation was identified in the spermatid-specific "capping protein (actin filament) muscle Z-line, alpha 3" gene (*Capza3*). CAPZA3 protein localization was altered in spermatids concurrent with altered localization of a unique CAPZB variant isoform and disruption of the filamentous actin (F-actin) network. These observations strongly suggest the missense mutation in *Capza3* is responsible for the mutant phenotype of *repro32/repro32* sperm and regulation of F-actin dynamics by a spermatogenic cell-specific CAPZ heterodimer is essential for removal of the cytoplasm and maintenance of midpiece integrity during spermiation in the mouse.

Keywords

testis; spermatid; spermatozoa; spermiogenesis; actin; ectoplasmic specialization; spermiation; tubulobulbar complex

Introduction

Spermiogenesis is the process during which spermatids undergo a series of complex morphological changes that result in formation of the highly specialized spermatozoon. In the mouse, as spermatids are remodeled from round (steps 1–8), to elongating (steps 9–12), and

*Correspondence: E. M. Eddy, NIEHS, NIH, 111 T.W. Alexander Drive, Research Triangle Park, NC 27709. FAX: 919-541-3800; E-mail: eddy@niehs.nih.gov.

then to condensing (steps 13–16), they form an acrosome, assemble a flagellum, and reshape and condense their nucleus (reviewed by Kerr et al., 2006). During this process, spermatids become attached to Sertoli cells by an apical ectoplasmic specialization (ES) consisting of a heterotypic adherens junction. The ES are underlain in the Sertoli cytoplasm by hexagonal arrays of F-actin bundles sandwiched between a cistern of endoplasmic reticulum and the plasma membrane. Proteins associated with the ES include F-actin, members of the laminin and integrin adhesion molecule families, and transmembrane actin-complex binding molecules, including nectins and CEACAM6 (Yan et al., 2006; Ozaki-Kuroda et al., 2002; Kurio et al., 2008).

Near the end of spermiogenesis much of the spermatid cytoplasm in shunted into a lobule that is detached during spermiation and remains behind to be phagocytosed by Sertoli cells (Russell, 1979b). A small amount of cytoplasm remains in the head and neck region and forms the cytoplasmic droplet, which moves to the midpiece-principal piece junction and usually is shed in the epididymis. Aberrant retention of excess cytoplasm by human sperm is associated with impaired sperm motility, increased reactive oxygen species (ROS) production and decreased in vitro fertilization (IVF) success, resulting in sub-fertility or infertility (reviewed by Cooper, 2005).

The mechanisms responsible for removal of spermatid cytoplasm during spermiation in mammals are unclear. However, filamentous actin (F-actin) has been shown to be involved in this process in insects (Noguchi et al., 2003; Sahara and Kawamura, 2004). The potential role (s) of F-actin during spermiogenesis in mammals have been inferred from morphological studies, and include involvement in shaping the acrosome (Welch and O'Rand, 1985), attachment of the acrosome to the spermatid nucleus (Russell et al., 1986), and/or removal of cytoplasm during spermiation (Russell, 1979a; Russell, 1979b). In support of the latter proposed role, intratesticular injection of cytochalasin D to depolymerize actin resulted in retention of excess cytoplasm by testicular sperm along with disruption of tubulobulbar complexes (TBCs). Intratesticular injection of taxol to disrupt microtubules did not alter removal of cytoplasm at spermiation (Russell et al., 1989).

Unbiased approaches for identification of mutant phenotypes can be helpful in the dissection of complex processes such as spermatid cytoplasmic remodeling. The present study was undertaken to identify the mutation responsible for the aberrant sperm phenotype and male infertility in *repro32* mice. The *repro32* mutation was produced by the Reproductive Genomics program at The Jackson Laboratory (http://reproductivegenomics.jax.org/), using random N-ethyl-N-nitrosourea (ENU) mutagenesis and a breeding strategy to identify recessive mutations affecting male and/or female fertility (Handel et al., 2006; Lessard et al., 2007). Spermiogenesis in *repro32/repro32* mice was abnormal and sperm were present in low concentrations in the epididymis, had abnormally shaped heads, exhibited poor motility, and showed very low IVF success. We identified a missense mutation in a spermatogenic cell-specific gene that is expressed solely in spermatids and encodes a protein involved in regulating F-actin dynamics. This study provides strong evidence that F-actin has an important role in removal of cytoplasm and maintenance of middle piece organization during spermiogenesis and spermiation, and that it is the disruption of F-actin organization during these processes that results in the structurally aberrant sperm and infertility of *repro32/repro32* male mice.

Materials and Methods

Mapping the repro32 mutation

The chromosomal localization of the *repro32* mutation was determined by genome scanning with a panel of polymorphic microsatellite markers that discriminate between C57BL/6 and C3H chromosomal regions. Genotyping was performed by PCR on DNA extracted from tail

tips of G3 progeny using standard conditions (Lessard et al., 2007). PCR products were analyzed on a 3% low EEO agarose (Fisher) gels. The map position was refined by breeding additional pairs of *repro32*/+ mice to generate offspring with recombinant chromosomes. The offspring were phenotyped by fertility testing and genotyped with additional polymorphic microsatellite markers to narrow the candidate region.

Tissue collection

All animal procedures were performed in accordance with the NRC Guide for the Care and Use of Laboratory Animals and approved by the Animal Care and Use Committees of the National Institute of Environmental Health Sciences (NIEHS) and The Jackson Laboratory. In vitro fertilization (IVF) assays were performed as described previously (Eppig and O'Brien, 1996). Animals were euthanized and weighed and then one testis was removed, weighed, and immediately snap-frozen in liquid nitrogen and stored at −80°C for later extraction of protein or RNA. The other testis was processed for histology or transmission electron microscopy as described previously (Miki et al., 2002). Sperm were collected by carefully dissecting cauda epididymides to remove blood vessels and fat, making several small cuts with iridectomy scissors and allowing the sperm to swim out into 1X PBS (Ca^{2+}/Mg^{2+}-free) at room temperature. Sperm were prepared for scanning electron microscopy (SEM) and demembranated in 1% Triton X-100 as described previously (Miki et al., 2002; Miki et al., 2004). Sperm counts were done using a hemocytometer.

Sequencing of candidate genes

Genomic DNA was isolated from tail tip biopsies of male *repro32*/+, *repro32*/*repro32*, and founder strain (C57/Bl6 and C3H) mice using the DNeasy kit (Qiagen) according to manufacturer's instructions. Primer pairs were designed to flank the exons of each of the candidate genes and PCR was used to amplify each exon and adjacent intronic sequence (sequences are available upon request). RNA was isolated from *repro32/repro32* testes using the RNeasy kit (Qiagen), and 1 μg total RNA was reverse-transcribed into cDNA using oligo dT primers and MuLV reverse transcriptase (Applied Biosystems). PCR and RT-PCR products were purified using the QIAquick PCR purification kit (Qiagen) and sequenced using Big Dye Version 3.1 (ABI) on an Avant 3100 sequencer (Applied Biosystems), both according to the manufacturers' instructions. The sequences obtained were identical to those in the public database.

Reverse transcriptase PCR (RT-PCR)

RNA was isolated using Trizol reagent (Invitrogen) according to the manufacturer's instructions, and cDNA was generated from 1 μg total RNA using oligo dT primers and MuLV reverse transcriptase (Applied Biosystems). 50 ng of cDNA was amplified for 35 cycles in a reaction containing: 10 mM Gene Amp PCR buffer II, 2 mM $MgCl_2$, 1.5 mM dNTPs, 1.25 μM of each primer, and 1.25 U Taq Gold (Perkin-Elmer). Primers used for amplification of the unique *Capzb_v3* 5′ end (upper F: 5′-ACACGATGCATCCTAGCAGGC, upper R: 5′-CAGATGACAGGAGATCTTCACAC), the 3′ end common to all three known *Capzb* isoforms (lower F: 5′-TGAGTGACTGTTCCCCACAC, lower R: 5′-TGCTGCTTTCTCTTCAAGGC), and for cytoplasmic *Actb* (F: 5′-TCCGATGCCCTGAGGCTCTTTTC, R: 5′-CTTGCTGATCCACTATCTGCTGGAA) were designed to span introns to control for possible amplification of genomic DNA.

Immunoblot analysis

Protein was extracted by homogenization of wild type and *repro32*/*repro32* testes as described previously (Goto and Eddy, 2004). Twenty μg of the insoluble fraction from whole testis extracts were boiled in SDS buffer for 10 minutes, separated on a 10% Tris-glycine gel

(Biorad), and immunoblotted using standard procedures. Antibodies to ACTB (A-5441, Sigma), CAPZA3 (GP-SH4, Progen), and CAPZB3 (GP-SH5, Progen) were used at 1:10,000, 1:1,500, and 1:500, respectively. Two additional polyclonal antisera to CAPZA3 were the kind gifts of Dr. Roy Jones, Babraham Institute and Dr. Hiromitsu Tanaka, Osaka University. HRP-conjugated goat-anti-mouse (for ACTB, from Sigma) and donkey-anti-guinea pig (for CAPZA3 and CAPZB, from Jackson Immuno) secondary antibodies were each used at 1:20,000. Detection was done using the ECL Plus Detection System (Amersham).

Indirect immunofluorescence (IIF) microscopy

Spermatids were prepared for immunostaining using a procedure modified from one described previously (Vogl et al., 1986). Briefly, *repro32*/+ and *repro32*/*repro32* mice were euthanized and their testes removed, decapsulated, and placed into cold 1X PBS. The tubules were gently teased apart and then incubated in the presence or absence of 1 mg/ml (0.1%) trypsin (Sigma) for 15 minutes at 33°C. The tubules were washed 3 times with 1X PBS, fixed in 4% paraformaldehyde (in 1X PBS, pH 7.2) for 10 minutes at room temperature, and washed 3 more times with 1X PBS. The remaining incubations were performed at room temperature in a humid chamber. Short (~1 mm) tubule segments were placed onto a Superfrost Plus positively charged slide (Fisher) and permeabilized with Automation buffer (Biomeda) for 10 minutes. Blocking was done for 20 minutes in Automation buffer containing 4.5% horse serum, and tubule segments were then incubated with primary antibody for 1 hour. Following three washes in 1X Automation buffer, tubules were incubated in secondary antibody with or without fluorescent dye-conjugated phalloidin-568 (Invitrogen) diluted 1:25 (yielding approximately 265 nM final concentration, or 1 unit/section) for 1 hour in the dark. Three additional washes in Automation buffer were performed in the dark, and coverslips were mounted using Vectashield containing DAPI (Vector Laboratories) and sealed with clear nail polish. For phalloidin-only labeling, tubule segments were incubated following permeabilization with phalloidin for 1 hour in the dark, washed, and mounted as above. Images were obtained using a Zeiss LSM 5 Pascal UV inverted laser scanning microscope with an Omnichrome argon-krypton laser and a Zeiss Plan-Apo 100 (1.4 na) oil immersion objective. Images were scanned and analyzed using LSM PASCAL version 3.2 software.

Statistical Analysis

Statistical analyses of body, testis, and seminal vesicle weights and of cauda epididymal sperm counts of *repro32/+* and *repro32/repro32* mice were conducted using Student's t-test. Differences were considered significant when $P<0.01$.

Results

Production of the repro32 mutation

Male C57BL/6J (herein designated B6) mice treated with ENU to produce point mutations were mated with C3HeB/FeJ (herein designated C3H) female mice to generate G1 progeny. The G1 male mice were mated with C3H female mice to produce G2 offspring, females of which were backcrossed to the G1 male to generate G3 progeny. Approximately 25% of the G3 mice were expected to be homozygous for any recessive mutation transmitted by the G1 male. The G3 mice were mated to wild type mice to identify infertility phenotypes (Handel et al., 2006; Lessard et al., 2007), which led to identification of the *repro32* mutation. Further mating of G2 females to the G1 male determined that approximately 25% of males derived from these backcrosses were infertile. This process confirmed that the recessive mutation was transmissible and generated mice for initial low-resolution gene mapping (see below).

Analysis of the repro32/repro32 phenotype

Initial analysis by the Reproductive Genomics Program found no apparent gross phenotypic differences between wild type, heterozygous (*repro32/+*), and homozygous (r*epro32/repro32*) mutant mice (http://reproductivegenomics.jax.org/mutants/G1-510-4.html). In addition, the sperm from *repro32/repro32* males had very low in vitro fertilization (IVF) capability in 7 separate experiments. Using sperm from 10 *repro32/repro32* males and scoring an average of 65 oocytes per male (range 26 to 118), a mean of 4.2% of eggs were found to proceed to the 2-cell stage. Using sperm from 7 C57BL/6J males and scoring an average of 73 oocytes per male (range 49–88), a mean of 75.5% of eggs proceeded to the 2-cell stage. We confirmed that the *repro32/repro32* males were infertile, had significantly decreased cauda epididymal sperm counts as compared to *repro32*/+ males ($P<0.01$), poor sperm motility (Table 1; Supplementary Movies), and abnormal sperm morphology (oligoasthenoteratozoospermia). The cauda epididymis contains a considerable amount of cell debris and sperm that are difficult to identify (Fig. S1). However, the general structure and organization of the seminiferous epithelium appeared normal until spermiogenesis, when abnormalities were apparent.

Condensed spermatids (step 16) become testicular sperm upon release during stage VIII of the seminiferous epithelium cycle. By stage IX, the seminiferous epithelium should contain only early elongating spermatids (step 9). However, both condensed spermatids and elongating spermatids were present during Stage IX in *repro32/repro32* mice (Fig. S2). By stage X in *repro32/repro32* mice, condensed spermatids were no longer present and the seminiferous epithelium appeared comparable to that in wild type mice (data not shown). Although condensed spermatids were retained, there were no overt differences in the appearance or orientation of early elongating spermatids (step 9) in *repro32/repro32* during stage IX tubules (Fig. S2).

During spermiogenesis, the outer dense fibers (ODFs) develop from proximal to distal around the microtubule-containing axoneme, the mitochondria migrate into the flagellum and surround the ODFs to form the midpiece, and the fibrous sheath develops from distal to proximal to delineate the principal piece (Irons and Clermont, 1982a; Irons and Clermont, 1982b). In the latter steps of these processes, most of the cytoplasm is redistributed from around the head and flagellum into a narrow-necked lobule that is shed during spermiation (Clermont et al., 1993). The first overt change in spermatogenic cells of *repro32/repro32* mice seen by transmission electron microscopy (TEM) was in late condensing spermatids (step 15–16), with a dramatic disruption of structural organization becoming apparent. The middle piece region of the flagellum was disorganized and its structural components surrounded the sperm head within an abnormal accumulation of cytoplasm (Fig. 1A and S3A), in contrast to what was observed in spermatids of wild type mice at the same stage (Fig. 1B). These features also were seen in *repro32/repro32* sperm in the cauda epididymis (Figs. 1C and S3B), but not in wild type sperm (Fig. 1D). Cytoplasmic droplets (CDs) were present at the junction of the midpiece and principal piece of the flagellum of a majority of sperm from the cauda epididymis of *repro32*/+ mice, but were absent from *repro32*/*repro32* sperm (Fig. 2 and Supplemental movies).

By scanning electron microscopy (SEM), the plasma membrane was seen to be closely applied to the head of wild type sperm (Fig. 3A), while a bag of cytoplasm loosely encased the head of *repro32*/*repro32* sperm (Fig. 3B). It was seen in *repro32/repro32* sperm demembranated by detergent treatment that ODF and other flagellar components were disorganized and wrapped around the sperm nucleus (Fig. 3D).

Mapping the repro32 phenotype and selection and sequencing of candidate genes

Genome scans using 2–3 polymorphic microsatellite markers per autosomal chromosome were performed on DNA from G3 progeny males. A region on Chr 6 between *D6Mit254* and *D6Mit14* homozygous for B6 genomic DNA in all infertile *repro32* males was identified as the candidate region for the ENU mutation. This was confirmed by further genotyping for polymorphic microsatellite markers flanking the candidate region. The *D6Mit254* and *D6Mit14* markers were used for subsequent progeny genotyping and colony maintenance. Matings were carried out between heterozygous progeny for several generations to produce additional Chr 6 recombinants. A total of 353 mice were genotyped for the flanking markers and 65 recombinant individuals were identified. Typing of the recombinant individuals for microsatellite markers within this region allowed narrowing of the candidate region for the *repro32* mutation to an 8-Mb genomic interval between *D6Mit291* and *D6Mit14*, defined by 11 independent recombination events.

The 8-Mb genomic interval on Chr 6 contains 43 known and 15 hypothetical genes. Searches of the literature, EST databases, and GEO profiles were used to identify candidate genes likely to be expressed exclusively or principally in spermatogenic cells. The number of genes potentially responsible for the *repro32* phenotype was reduced by excluding genes that were: 1) knocked out by gene targeting [14 genes], 2) knocked down by transgenic RNAi [1 gene] (Knott et al., 2005), 3) not expressed in the testis [13 genes], or 4) expressed in numerous tissues [11 genes]. The knocked out or knocked down genes were excluded because the phenotype produced was unlike the *repro32* phenotype. Four genes (*Igbp1b*, *Tuba3b*, *Ifltd1* and *Capza3*) remained as candidates based on these exclusion criteria. Exons and intron-exon junctions of *Igbp1b*, *Tuba3b*, and *Capza3* were sequenced using genomic DNA isolated from tail tissue of *repro32*/*repro32* male mice, while *Ifltd1* was amplified and then sequenced from both genomic DNA from tail tissue and *repro32/repro32* testis cDNA.

Mutations were not found in *Igbp1b*, *Tuba3b*, or *Ifltd1*, but an A/T nucleotide transversion resulting in a methionine-to-lysine missense mutation (M44K) was found in the gene for "capping protein (actin filament) muscle Z-line, alpha3" (*Capza3;* UniGene Mm.12817) in *repro32/repro32* mice. CAPZA functions in somatic cells as a heterodimer with a CAPZB subunit to form a functional CAPZ complex capable of binding to the barbed ends of actin filaments with high affinity and preventing the addition or loss of actin subunits (Wear and Cooper, 2004). The mutation was confirmed by sequencing DNA from the B6 and C3H parental strains (Fig. 4A). The *Capza3* gene lacks introns and encodes a 298 amino acid protein shown by northern analysis (Tanaka et al., 1994) and UniGene EST profiles (http://www.ncbi.nlm.nih.gov/UniGene/ESTProfileViewer.cgi?uglist=Mm.12817) to be expressed specifically in testis and by microarray analysis data to be expressed specifically in spermatids (Shima et al., 2004; http://mrg.gs.washington.edu/index.cgi?mrg_id=85248). The CAPZA3 protein is highly conserved, with at least 90% identity and 96% similarity at the amino acid level occurring in 7 eutherian mammals for which the CAPZA3 sequence has been determined. The M44K substitution in CAPZA3 of *repro32* mutant mice occurred in a 39 amino acid region with 100% identity in these species (Fig. 4B).

CAPZA3 protein expression and localization in repro32/+ and repro32/repro32 spermatids

There were no apparent differences in the amount of CAPZA3 in the insoluble fraction of lysates from testes of *repro32/repro32* and wild type mice (Fig. 5C). In *repro32/+* spermatids, CAPZA3 was detectable first in a narrow arc at the periphery of the developing acrosome in step 8 round spermatids (Fig. 5A.i). It surrounded the acrosome in elongating (Fig. 5A.ii) and early condensing spermatids (Fig. 5A.iii) and localized mainly in the post-acrosomal region of the sperm head in late condensing spermatids (Fig. 5A.iv). This pattern persisted in testicular and epididymal spermatozoa, which is consistent with the distribution of CAPZA3 seen in rat

spermatids and testicular spermatozoa (Hurst et al., 1998) and in human spermatozoa (Miyagawa et al., 2002).

The localization of CAPZA3 in round spermatids from *repro32*/*repro32* mice was similar to that in *repro32*/+ mice (Fig. 5B.i). However, in elongating spermatids it remained associated mainly with the convex margin of the acrosome (Fig. 5B.ii) and in condensing spermatids it failed to achieve the consistent pattern of localization seen in *repro32*/+ mice (Fig. 5B.iii–vi). The altered localization of CAPZA3 in isolated elongating and condensing spermatids from *repro32*/*repro32* mice preceded the appearance of the overt mutant phenotype seen by TEM (Fig. 1A). The results shown were obtained with a commercial CAPZA3 antiserum (GP-SH4), but similar results were observed with antisera to CAPZA3 kindly provided by Drs. Jones and Tanaka (data not shown).

A novel CAPZB isoform is present in mouse spermatids

Because CAPZA forms a complex with CAPZB in somatic cells, CAPZB was investigated in wild type and *repro32*/*repro32* mice. Two well-characterized mouse CAPZB isoforms are expressed in muscle or ubiquitously and are products of alternative transcripts from the *Capzb* gene on Chr 4 (Schafer et al., 1994). A third CAPZB isoform isolated from bovine sperm is the product of another alternative transcript abundant in testis and detectable in brain (von Bülow et al. 1997). An RT-PCR fragment generated from mouse brain cDNA had high identity with a region of this bovine sequence (von Bülow et al. 1997).

To determine which CAPZB isoforms are present in mouse testis, RT-PCR was performed with primers designed from the sequences of the two known alternative transcripts (*Capzb_v1* and *Capzb_v2*) (Fig. 6A). The *Capzb_v2* transcript differs from *Capzb_v1* due to an alternative splicing event that removes 113 nucleotides within the C-terminal exon (Schafer et al., 1994). *Capzb_v1* was identified in cDNA from skeletal muscle and at a very low level in Sertoli cells, while the *Capzb_v2* sequence was distributed more widely (Fig. 6B). The possible presence of *Capzb_v3* in the mouse testis was investigated at selected ages from 15 to >60 days post partum (dpp) using a primer set with the 5′ primer located within the mouse sequence corresponding to the bovine gene alternative first exon (von Bülow et al., 1997) (labeled 1b, Fig. 6A). A *Capzb_v3* sequence was first detected on day 22, coinciding with the first wave of round spermatid development. Using these primers and RNA isolated from highly enriched populations of germ cells (a gift of Dr. John McCarrey, University of Texas at San Antonio), *Capzb_v3* transcripts were detected in round spermatids, but not in pachytene spermatocytes or in the other mouse tissues examined (Fig. 6B). These amplification products were sequence-verified (data not shown), and confirmed the predicted usage of an alternate exon 1 (von Bülow et al. 1997) downstream of somatic exon 1 as well as exon 9 from *Capzb_v2* (Fig. 6A). Therefore, the isoform encoded by mouse *Capzb_v3* (referred to hereafter as CAPZB3) differs from the other CAPZB isoforms by the presence of an N-terminal extension resulting from utilization of an alternative first exon and is detectable only in round spermatids (GenBank accession no. **FJ692320**).

The CAPZB3 isoform was characterized using antisera specific to its unique N-terminal extension. Immunoblot analysis determined that a protein of approximately 36 kDa (predicted = 33.8 kDa) was present in the insoluble portion of lysates of whole testis from wild type mice (Fig. 5C). Spermatids were isolated mechanically and treated with trypsin to remove Sertoli cell remnants and examined by indirect immunofluorescence microscopy to determine the location of CAPZB3. The localization pattern of CAPZB3 was similar to CAPZA3 in elongating and condensing spermatids (data not shown) and in testicular sperm from *repro32*/+ mice (Fig. 6C). We found that CAPZB3 protein distribution was altered in spermatids concurrently with the alteration of CAPZA3 (Fig. 5A) in elongating and condensing spermatids (data not shown) and in testicular sperm from *repro32/repro32* mice (Fig. S4A.i–

ii). Because CAPZA and CAPZB function as heterodimers in somatic cells, we postulate that CAPZA3 and CAPZB3 form a novel spermatid-specific CAPZ heterodimer.

F-actin organization is disrupted in repro32/repro32 condensing spermatids

The role of the CAPZ complex in regulating actin filament growth (reviewed by dos Remedios et al., 2003) and the spermatid-specific expression of *Capza3* in the mouse (Tanaka et al., 1994; Yoshimura et al., 1999) and rat (Hurst et al., 1998) suggested that a mutation in CAPZA3 would lead to perturbation of F-actin structures in *repro32*/*repro32* spermatids. Bundles of F-actin are seen at two sites in the luminal region of the mouse seminiferous epithelium. One is within the Sertoli cell ES, which is composed of closely packed F-actin filaments and a cistern of endoplasmic reticulum. The ES is present in the cytoplasm adjacent to junctional complexes that anchor developing spermatids to Sertoli cells (Russell, 1977). This complex also has been implicated in spermatid translocation within the seminiferous epithelium prior to spermiation (reviewed by Vogl et al., 2000). The ES F-actin organization was examined using phalloidin on mechanically isolated spermatids to which Sertoli cell remnants remained attached. No differences in ES F-actin fiber quantity, orientation, or appearance were apparent between spermatids from *repro32/+* and *repro32/repro32* mice (Fig. 7A–B), and the patterns were similar to those reported previously (Vogl et al., 1985; Young et al., 2008).

The other location where F-actin is seen is within developing spermatids. To view the F-actin in spermatids unobscured by Sertoli cell ES F-actin, seminiferous tubules were mechanically disrupted and incubated with trypsin to separate Sertoli cell remnants from developing spermatids (Vogl et al., 1986; Masri et al., 1987) prior to fixation and labeling with phalloidin. The ES removed from condensing spermatids can be seen after trypsin treatment (Fig. S5A–C). The F-actin fibers first became detectable within round spermatids (~step 8) as a band between the cell surface and the developing acrosome (Fig. 8A.i). In elongating spermatids (steps 9–12), F-actin is present in a crescent overlying the convex aspect of the acrosomal region (Fig. 8A.ii), and in condensing spermatids (~step 13) the crescent begins to resolve into a distinct band along the convex margin with a diffuse accumulation over the lateral aspect of the acrosomal region (Fig. 8A.iii). The F-actin in late condensing spermatids (steps 14–16) was seen in a distinct band along the convex margin and dispersed unevenly over the lateral aspect of the acrosomal region (Fig. 8A.iv). However, F-actin was no longer detectable with phalloidin in testicular (Fig. 8A.v) or epididymal sperm (data not shown), consistent with observations in other studies (e.g., Halenda et al., 1987; Flaherty et al., 1986).

The distribution of F-actin fibers in round spermatids from *repro32*/*repro32* mice was similar to those from *repro32*/+ mice, although they appeared thinner and shorter (Fig. 8B.i). The differences become more apparent in elongating spermatids, with the F-actin fibers being fewer, shorter, and more tangled in *repro32*/*repro32* mice and located more towards the anterior-dorsal portion of the head (Fig. 8B.ii) than in elongating spermatids from *repro32/+* mice (Fig. 8A.ii). Despite the differences in F-actin distribution in elongating spermatids from *repro32/repro32* and *repro32/+* mice, their overall morphological appearances were comparable. Differences became apparent at the TEM level during spermiation, after differences were seen in F-actin organization between *repro32/repro32* (Figs. 8B.iii–vi) and *repro32/+* spermatids (Figs. 8A.iii–v). However, the shape of nuclei in spermatids and sperm of *repro32/repro32* mice did not differ significantly from those of wild type mice, suggesting that F-actin does not have a major role in shaping the mouse sperm nucleus (Fig. 7A & 7B).

Discussion

This study identified a missense mutation in the *Capza3* gene in *repro32* mice produced by ENU mutagenesis and a screening protocol to discover mutations causing infertility. The mutant phenotype was inherited by *repro32* offspring in the expected Mendelian ratios and the

mutation was found using a candidate gene sequencing approach. CAPZA3 mislocalization occurred in condensing spermatids coincident with mislocalization of CAPZB3 and disruption of the F-actin network. The *repro32/rero32* spermatids failed to shed excess cytoplasm during spermiation and the axoneme, mitochondria, and ODFs of the middle piece were present in a tangled array within a bag of cytoplasm surrounding the sperm head.

A point mutation is present in the Capza3 gene of repro32 mice

ENU mutagenesis provides a powerful and nonbiased forward genetics approach to identify novel genes involved in male and female infertility (Harris et al., 2007; Ward et al., 2007; Philipps et al., 2008). The missense mutation in *Capza3* was identified by sequencing exons and exon-intron junctions of candidate genes. While there remains a possibility that an additional mutation might contribute to the phenotype, the combined results from 4 studies suggest there is less than a 5% likelihood of another mutation occurring in the 8-Mb critical region (Keays et al., 2006). However, we expect the likelihood of another mutation causing the *repro32* phenotype to be considerably less than 5% because mutations in exons may be silent and much of the 8-Mb region consists of intragenic and intronic sequence.

A recent study identified 4 QTLs involved in controlling sperm head shape (L'Hôte et al., 2007). One of these (*Sh1*) mapped to the region on chromosome 6 containing *Capza3* and three other testis-specific genes (*Igpb1b*, *Plcz1*, and *Tuba3b*) identified as potential candidate genes affecting the trait. However, the abnormal phenotype associated with the head-shape QTLs was a hammerhead shaped sperm nucleus, while the nuclear shape in *repro32/repro32* sperm is relatively normal, suggesting that *Capza3* alone cannot determine the head shape trait defined by the QTLs. However, it is possible that different *Capza3* alleles and/or interactions with genes in the other QTLs are associated with the trait.

The spermatid-specific F-actin capping protein complex

The CAPZA and CAPZB heterodimer (CAPZ) regulates actin dynamics by preventing addition or loss of G-actin subunits to the fast-growing or barbed end of F-actin fibers (reviewed by dos Remedios et al., 2003; Wear and Cooper, 2008). Previous studies determined the intronless *Capza3* gene encodes a testis-specific isoform of CAPZA that is expressed in spermatids in mouse (Tanaka et al., 1994; Yoshimura et al., 1999) and rat (Hurst et al., 1998), and a testis-specific isoform of CAPZB is present in bull sperm (von Bülow et al., 1997). The current studies: 1) confirmed *Capza3* gene expression is confined to spermatids, 2) demonstrated the *Capzb_v3* variant transcript and CAPZB3 protein are expressed in spermatids, 3) determined the CAPZA3 and CAPZB3 proteins are present in spermatids and sperm, 4) demonstrated F-actin filaments are present in spermatids but not in sperm of the mouse, as is seen in other species (Welch and O'Rand, 1985; Vogl et al., 1986; Halenda et al., 1987), and 5) observed that F-actin, CAPZA3 and CAPZB3 are found in the same cytoplasmic regions in condensing and elongating spermatids. Taken together, these results strongly suggest that a spermatid-specific CAPZA3/CAPZB3 heterodimer plays a significant role in regulating F-actin dynamics in condensing and elongating spermatids.

CAPZ and F-actin organization in repro32/repro32 spermatids

We have shown the organization and distribution of CAPZA3, CAPZB3, and F-actin is disrupted in condensing and elongating spermatids of *repro32/repro32* mice. The M44K missense mutation occurs in the N-terminal portion of CAPZA3 with nearly 100% identity among the eutherian mammals for which the sequence is known. This implies the novel N-terminal region imparts a conserved spermatid-specific function, interaction, or localization for CAPZA3 that would be subject to disruption by the substitution of a positively charged lysine for a hydrophobic methionine.

There are several possibilities for how the missense mutation in CAPZA3 would result in the mutant sperm phenotype: 1) Substitution of a positively charged lysine for a hydrophobic methionine (M44K) might disrupt the tertiary structure of CAPZA3. Because misfolded proteins often are targeted to the proteasome for elimination (reviewed by Goldberg and Dice, 1974), we examined CAPZA3 protein levels by immunoblot analysis. However, there was no apparent difference in the amount of CAPZA3 in lysates of testes from wild type and *repro32/repro32* mice; 2) CAPZA3 and CAPZB3 have novel N-terminal regions and the M44K mutation might disrupt assembly of the CAPZ heterodimer or its interaction with F-actin. Arguing against this is the finding that the N-terminus of chicken CAPZA1 is not required to dimerize with CAPZB or to bind F-actin (Casella and Torres, 1994); 3) The novel CAPZA3 and CAPZB3 N-terminal regions might target or anchor CAPZ in spermatids. In addition, novel N-terminal regions are a common feature of spermatid- and sperm-specific proteins and are thought to be involved in localizing or anchoring these proteins (e.g., Vemuganti et al., 2007). Although we favor the latter possibility for how the missense mutation in CAPZA3 produces the *repro32/repro32* sperm phenotype, the results are correlative and further studies will be needed to define the effects of the substitution of a lysine for a methionine on the structure and/or function of CAPZA3.

The role of F-actin in spermatid cytoplasm removal

It previously was hypothesized that up to 70% of the spermatid cytoplasmic fluid volume is taken up by Sertoli cells through the TBC (Russell, 1979b; Russell and Malone, 1980). Most of the remaining cytoplasm is pinched off during spermiation to form the residual body that is phagocytosed by Sertoli cells (reviewed by Kerr et al., 2006. A small amount of cytoplasm remaining at the junction of the sperm head and neck becomes the cytoplasmic droplet that moves down the sperm flagellum as sperm traverse the epididymis (reviewed by Cooper, 2005).

An abnormal retention of cytoplasm can be seen by TEM in step 15–16 *repro32/repro32* condensing spermatids in the region that will become the head and neck of the sperm. In addition, a greater than normal amount of cytoplasm remains associated with *repro32/repro32* sperm following spermiation. Typical residual bodies are not apparent in the seminiferous epithelium, but vesicles are abundant in the epididymis (Supplementary Movie) and may represent residual cytoplasm shed from sperm after spermiation, as well as cytoplasm-encased sperm heads. Cytoplasmic droplets (CDs) present on most wild type and *repro32*/+ cauda epididymal sperm are absent from *repro32*/*repro32* sperm. If the hypothesis for cytoplasmic fluid removal is correct, disruption of F-actin distribution or function in *repro32/repro32* condensing spermatids might result in defective TBC function as well as disruption of cytoplasmic removal at spermiation.

The results of this study suggest: 1) the *repro32* phenotype is caused by a missense mutation in the *Capza3* gene, 2) CAPZA3 is required for maintenance of male fertility in the mouse and probably other mammalian species, 3) a novel CAPZA3/CAPZB3 heterodimer regulates F-actin dynamics in spermatids, 4) F-actin has an essential role in formation and stabilization of the nascent spermatozoon, and 5) F-actin does not have a major role in shaping the sperm head. They also raise the question of what roles are served by the novel N-terminal regions of CAPZA3 and CAPZB3. Finally, it should be noted that testis-specific genes expressed in spermatids have been identified for the actin-like proteins ACTL7A and ACTL7B (Tanaka et al., 2003) and actin-related proteins ACTRT1 and ACTRT2 (Heid et al., 2002) and it remains to be determined if they also serve roles in spermiogenesis and spermiation.

Supplementary Material

Refer to Web version on PubMed Central for supplementary material.

Acknowledgments

We would like to extend our sincere appreciation to Drs. Fanny Odet and Lisa Chadwick for helpful discussions, Gina Goulding and Linwood Koonce for technical assistance, and to Drs. John Schimenti and Jason Mercer for critical reading of the manuscript. This research was supported in part by the Intramural Research Program of the NIH, National Institute of Environmental Health Sciences (ZO1-ES070076, EME) and a grant from NIH, NICHD (PO1 HD-42137, MAH).

References

Beier DR, Herron BJ. Genetic mapping and ENU mutagenesis. Genetica 2004;122:65–69. [PubMed: 15619962]

Casella JF, Torres MA. Interaction of Cap Z with actin. The NH2-terminal domains of the alpha 1 and beta subunits are not required for actin capping, and alpha 1 beta and alpha 2 beta heterodimers bind differentially to actin. J Biol Chem 1994;269(9):6992–6998. [PubMed: 8120062]

Clermont, Y.; Oko, R.; Hermo, L. Cell biology of mammalian spermiogenesis. In: Desjardins, C.; Ewing, LL., editors. Cell and Molecular Biology of the Testis. Oxford University Press; New York: 2003. p. 332-376.

Cooper TG. Cytoplasmic droplets: the good, the bad, or just confusing? Hum Reprod 2005;20:9–11. [PubMed: 15471925]

dos Remedios CG, Chhabra D, Kekic M, Dedova IV, Tsubakihara M, Berry DA, Nosworthy NJ. Actin binding proteins: regulation of cytoskeletal microfilaments. Physiol Rev 2003;83:433–473. [PubMed: 12663865]

Eppig JJ, O'Brien MJ. Development in vitro of mouse oocytes from primordial follicles. Biol Reprod 1996;54:197–207. [PubMed: 8838017]

Flaherty SP, Winfrey VP, Olson GE. Localization of actin in mammalian spermatozoa: a comparison of eight species. Anat Rec 1986;216:504–515. [PubMed: 2432804]

Goldberg AL, Dice JF. Intracellular protein degradation in mammalian and bacterial cells. Ann Rev Biochem 1974;43:835–869. [PubMed: 4604628]

Goto M, Eddy EM. Speriolin is a novel spermatogenic cell-specific centrosomal protein associated with the seventh WD motif of Cdc20. J Biol Chem 2004;279(40):42128–42138. [PubMed: 15280373]

Halenda RM, Primakoff P, Myles DG. Actin filaments, localized to the region of the developing acrosome during early stages, are lost during later stages of guinea pig spermiogenesis. Biol Reprod 1987;36:491–499. [PubMed: 2437971]

Handel MA, Lessard C, Reinholdt L, Schimenti J, Eppig JJ. Mutagenesis as an unbiased approach to identify novel contraceptive targets. Mol Cell Endo 2006;250:201–205.

Harris T, Marquez B, Suarez S, Schimenti J. Sperm motility defects and infertility in male mice with a mutation in *Nsun7*, a member of the Sun domain-containing family of putative RNA methyltransferases. Biol Reprod 2007;77:376–382. [PubMed: 17442852]

Hart MC, Cooper JA. Vertebrate isoforms of actin capping protein B have distinct functions in vivo. J Cell Biol 1999;147:1287–1298. [PubMed: 10601341]

Heid H, Figge U, Kuhn C, Zimbelmann R, Franke WW. Novel actin-related proteins Arp-T1 and Arp-T2 as components of the cytoskeletal calyx of the mammalian sperm head. Exp Cell Res 2002;279:177–187. [PubMed: 12243744]

Hurst S, Howes EA, Coadwell J, Jones R. Expression of a testis-specific putative actin-capping protein associated with the developing acrosome during rat spermiogenesis. Mol Reprod Dev 1998;49:81–91. [PubMed: 9406198]

Irons MJ, Clermont Y. Formation of the outer dense fibers during spermiogenesis in the rat. Anat Rec 1982a;202(4):463–471. [PubMed: 7200337]

Irons MJ, Clermont Y. Kinetics of fibrous sheath formation in the rat spermatid. Am J Anat 1982b;165 (2):121–130. [PubMed: 6890760]

Keays DA, Clark TG, Flint J. Estimating the number of coding mutations in genotypic- and phenotypic-driven N-ethyl-nitrosourea (ENU) screens. Mamm Genome 2006;17:230–238. [PubMed: 16518690]

Kerr, JB.; Loveland, KL.; O'Bryan, MK.; de Krester, DM. Cytology of the testis and intrinsic control mechanisms. In: Neill, JD., editor. Physiology of Reproduction, Third Edition. Elsevier Academic Press; St. Louis: 2006. p. 827-947.

Knott JG, Kurokawa M, Schultz RM, Williams CJ. Transgenic RNA interference reveals role for mouse sperm phospholipase C zeta in triggering Ca^{2+} oscillations during fertilization. Biol Reprod 2005;72 (4):992–996. [PubMed: 15601914]

Kurio H, Murayama E, Kaneko T, Shibata Y, Inai T, Iida H. Intron retention generates a novel isoform of CEACAM6 that may act as an adhesion molecule in the ectoplasmic specialization structures between spermatids and Sertoli cells in rat testis. Biol Reprod 2008;79(6):1062–1073. [PubMed: 18685128]

L'Hote D, Serres C, Laissue P, Oulmouden A, Rogel-Gaillard C, Montagutelli X, Vaiman D. Centimorgan-range one-step mapping of fertility traits using interspecific recombinant congenic mice. Genetics 2007;176:1907–1921. [PubMed: 17483418]

Lessard C, Lothrop H, Schimenti JC, Handel MA. Mutagenesis-generated mouse models of human infertility with abnormal sperm. Hum Reprod 2007;22:159–166. [PubMed: 16920728]

Masri BA, Russell LD, Vogl AW. Distribution of actin in spermatids and adjacent Sertoli cell regions of the rat. Anat Rec 1987;218:20–26. [PubMed: 3605657]

Miki K, Willis WD, Brown PR, Goulding EH, Fulcher KD, Eddy EM. Targeted disruption of the *Akap4* gene causes defects in sperm flagellum and motility. Dev Biol 2002;248(2):331–342. [PubMed: 12167408]

Miki K, Qu W, Goulding EH, Willis WD, Bunch DO, Strader LF, Perreault SD, Eddy EM, O'Brien DA. Glyceraldehyde 3-phosphate dehydrogenase-S, a sperm-specific glycolytic enzyme, is required for sperm motility and male fertility. Proc Natl Acad Sci 2004;101(47):16501–16506. [PubMed: 15546993]

Miyagawa Y, Tanaka H, Iguchi N, Kitamura K, Nakamura Y, Takahashi T, Matsumiya K, Okuyama A, Nishimune Y. Molecular cloning and characterization of the human orthologue of male germ cell-specific actin capping protein alpha 3 (cp alpha 3). Mol Hum Reprod 2002;8:531–539. [PubMed: 12029070]

Noguchi T, Miller KG. A role for actin dynamics in individualization during spermatogenesis in *Drosophila melanogaster*. Development 2003;130:1805–1816. [PubMed: 12642486]

Ozaki-Kuroda K, Nakanishi H, Ohta H, Tanaka H, Kurihara H, Mueller S, Irie K, Ikeda W, Sakai T, Wimmer E, Nishimune Y, Takai Y. Nectin couples cell-cell adhesion and the actin scaffold at heterotypic testicular junctions. Curr Biol 2002;12(13):1145–1150. [PubMed: 12121624]

Philipps DL, Wigglesworth K, Hartford SA, Sun F, Pattabiraman S, Schimenti K, Handel MA, Eppig JJ, Schimenti JC. The dual bromodomain and WD repeat-containing mouse protein BRWD1 is required for normal spermiogenesis and the oocyte-embryo transition. Dev Biol 2008;317:72–82. [PubMed: 18353305]

Russell LD. Observations on rat Sertoli ectoplasmic ('junctional') specializations in their association with germ cells of the rat testis. Tissue Cell 1977;9:475–498. [PubMed: 929577]

Russell LD. Further observations on tubulobulbar complexes formed by late spermatids and Sertoli cells in the rat testis. Anat Rec 1979a;194:213–232. [PubMed: 464323]

Russell LD. Spermatid-Sertoli tubulobulbar complexes as devices for elimination of cytoplasm from the head region of late spermatids of the rat. Anat Rec 1979b;194:233–246. [PubMed: 464324]

Russell WL, Kelly EM, Hunsicker PR, Bangham JW, Maddux SC, Phipps EL. Specific locus test shows ethylnitrosurea to be the most potent mutagen in the mouse. Proc Natl Acad Sci 1979;76:5818–5819. [PubMed: 293686]

Russell LD, Malone JP. A study of Sertoli-spermatid tubulobulbar complexes in selected mammals. Tissue Cell 1980;12:263–285. [PubMed: 6998046]

Russell LD, Weber JE, Vogl AW. Characterization of filaments within the subacrosomal space of rat spermatids during spermiogenesis. Tissue Cell 1986;18:887–898. [PubMed: 3810637]

Russell LD, Saxena NK, Turner TT. Cytoskeletal involvement in spermiation and sperm transport. Tissue Cell 1989;21:361–379. [PubMed: 2479117]

Sahara K, Kawamura N. Roles of actin networks in peristaltic squeezing of sperm bundles in *Bombyx mori*. J Morphol 2004;259:1–6. [PubMed: 14666520]

Schafer DA, Korshunova YO, Schroer TA, Cooper JA. Differential localization and sequence analysis of capping protein beta-subunit isoforms of vertebrates. J Cell Biol 1994;127(2):453–465. [PubMed: 7929588]

Shima JE, McLean DJ, McCarrey JR, Griswold MD. The murine testicular transcriptome: characterizing gene expression in the testis during the progression of spermatogenesis. Biol Reprod 2004;71(1): 319–330. [PubMed: 15028632]

Tanaka H, Iguchi N, Egydio de Carvalho C, Tadokoro Y, Yomogida K, Nishimune Y. Novel actin-like proteins T-ACTIN1 and T-ACTIN2 are differentially expressed in the cytoplasm and nucleus of mouse haploid germ cells. Biol Reprod 2003;69:475–482. [PubMed: 12672658]

Tanaka H, Yoshimura Y, Nishina Y, Nozaki M, Nojima H, Nishimune Y. Isolation and characterization of cDNA clones specifically expressed in testicular germ cells. FEBS Lett 1994;355:4–10. [PubMed: 7957958]

Vemuganti SA, Bell TA, Scarlett CO, Parker CE, de Villena FP, O'Brien DA. Three male germline-specific aldolase A isozymes are generated by alternative splicing and retrotransposition. Dev Biol 2007;309:18–31. [PubMed: 17659271]

Vogl AW, Grove BD, Lew GJ. Distribution of actin in Sertoli cell ectoplasmic specializations and associated spermatids in the ground squirrel testis. Anat Rec 1986;215:331–341. [PubMed: 3526980]

Vogl AW, Pfeiffer DC, Mulholland D, Kimel G, Guttman J. Unique and multifunctional adhesion junctions in the testis: ectoplasmic specializations. Arch Histol Cytol 2000;63:1–15. [PubMed: 10770585]

von Bülow M, Rackwitz HR, Zimbelmann R, Franke WW. CPB3, a novel isoform of an actin-binding protein, is a component of the cytoskeletal calyx of the mammalian sperm head. Exp Cell Res 1997;233:216–224. [PubMed: 9184090]

Ward JO, Reinholdt LG, Motley WW, Niswander LM, Deacon DC, Griffin LB, Langlais KK, Backus VL, Schimenti KJ, O'Brien MJ, Eppig JJ, Schimenti JC. Mutation in mouse hei10, an e3 ubiquitin ligase, disrupts meiotic crossing over. PLoS Genet 2007;3:e139. [PubMed: 17784788]

Wear MA, Cooper JA. Capping protein: new insights into mechanism and regulation. Trends Biochem Sci 2004;29(8):418–428. [PubMed: 15362226]

Welch JE, O'Rand MG. Identification and distribution of actin in spermatogenic cells and spermatozoa of the rabbit. Dev Biol 1985;109:411–417. [PubMed: 3996756]

Yan HH, Mruk DD, Lee WM, Cheng CY. Ectoplasmic specialization: a friend or foe of spermatogenesis? BioEssays 2006;29:36–48. [PubMed: 17187371]

Yoshimura Y, Tanaka H, Nozaki M, Yomogida K, Shimamura K, Yasunaga T, Nishimune Y. Genomic analysis of male germ cell-specific actin capping protein alpha. Gene 1999;237:193–199. [PubMed: 10524250]

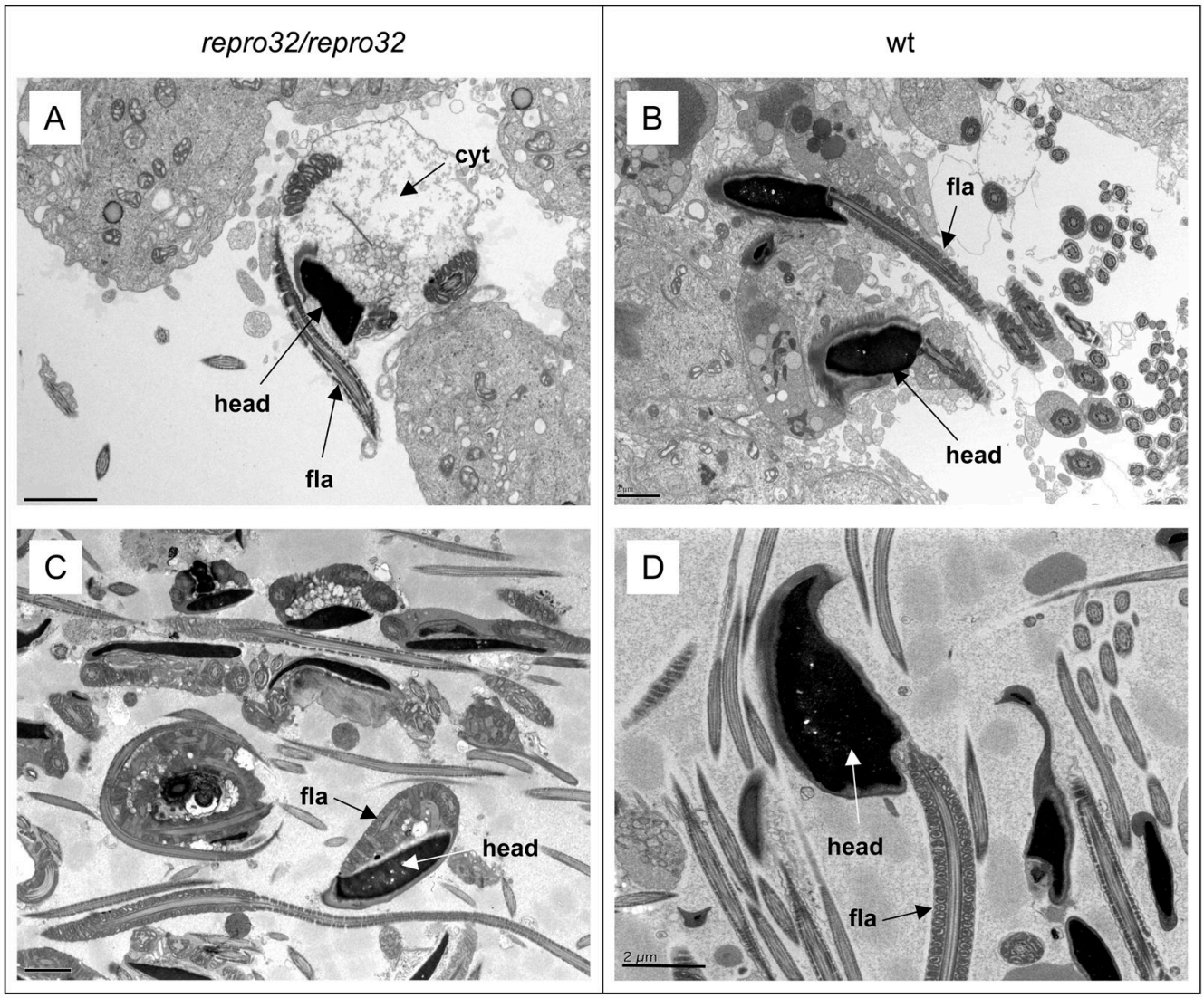

Figure 1.

Transmission electron microscopy (TEM) of the seminiferous epithelium and sperm in the cauda epididymis of *repro32*/*repro32* and wild type mice. (A) Condensing spermatids (step 16) of *repro32/repro32* and (B) wild type mice with the flagellum (fla) and cytoplasm (cyt) positioned for release from the seminiferous epithelium into the lumen of the tubule. (C) Sperm in the lumen of the cauda epididymis of *repro32/repro32* and (D) wild type mice. Scale bar = 2 μ.

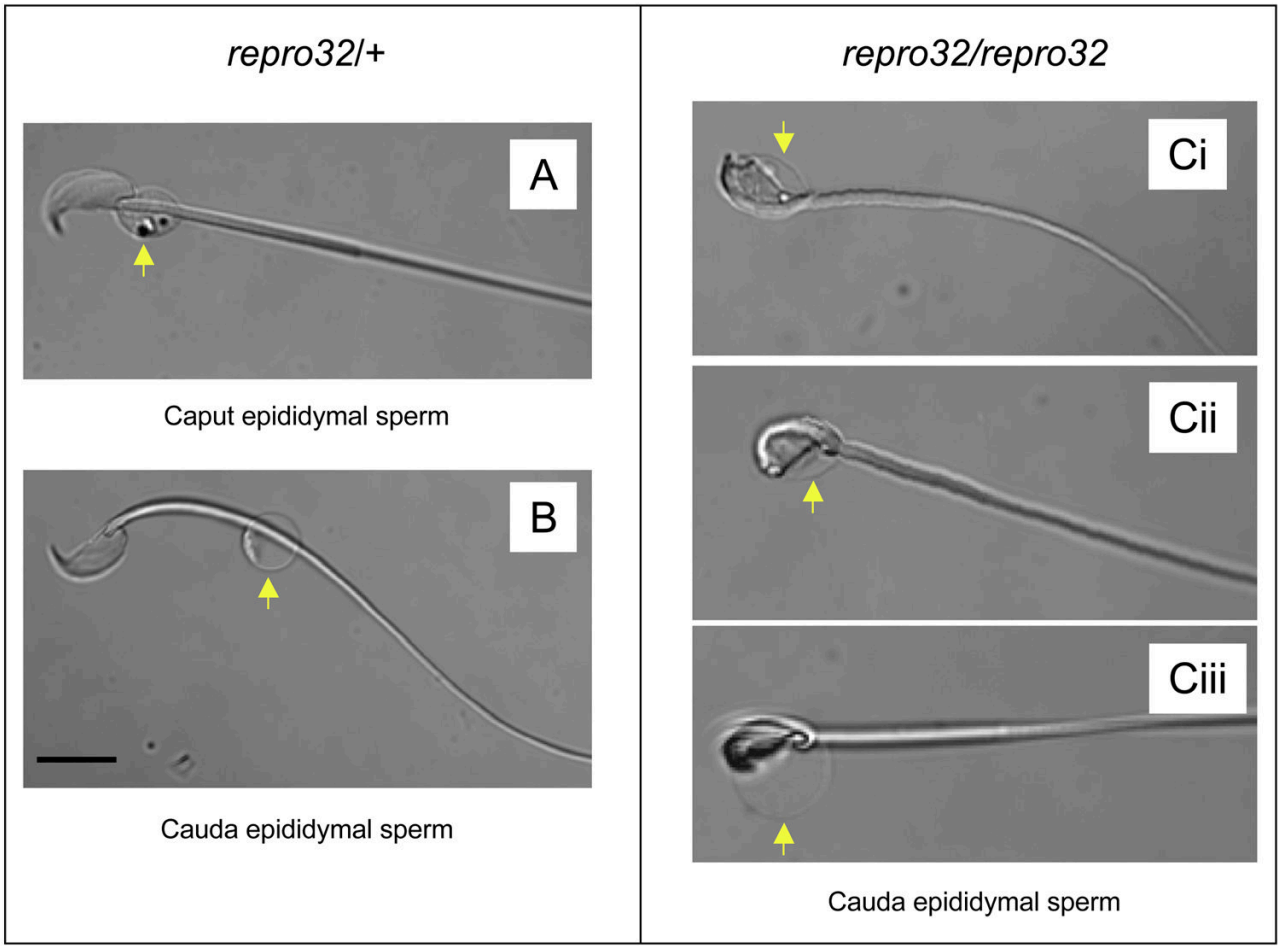

Figure 2.
Cytoplasmic droplet (CD) localization in *repro32*/+ and *repro32*/*repro32* sperm. (A, B) Differential interference contrast (DIC) images of *repro32*/+ sperm from the caput (A) and cauda (B) epididymis, with arrows indicating the locations of CDs. (C.i–iii) Examples of *repro32/repro32* sperm from the cauda epididymis with their head and neck regions enclosed within a bag of cytoplasm (indicated by arrows). Scale bar = 5 μ.

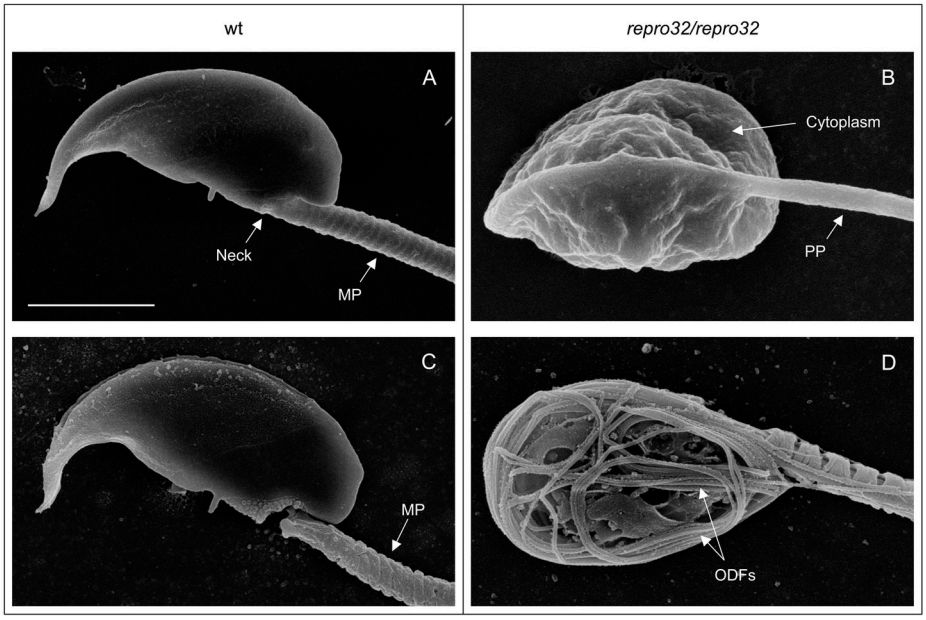

Figure 3.

Scanning electron microscopy (SEM) of cauda epididymal sperm from wild type and *repro32/repro32* mice. (A) A wild type mouse sperm, showing the head, neck and proximal part of the middle piece (MP). (B) A *repro32/repro32* mouse sperm with the head and MP enclosed within a bag of cytoplasm and the principal piece (PP) of the flagellum visible. (C) A wild type mouse sperm demembranated by detergent treatment. (D) A *repro32/repro32* demembranated mouse sperm, showing the outer dense fibers (ODFs) and the middle piece wrapped around the sperm head. Scale bar = 2 μ.

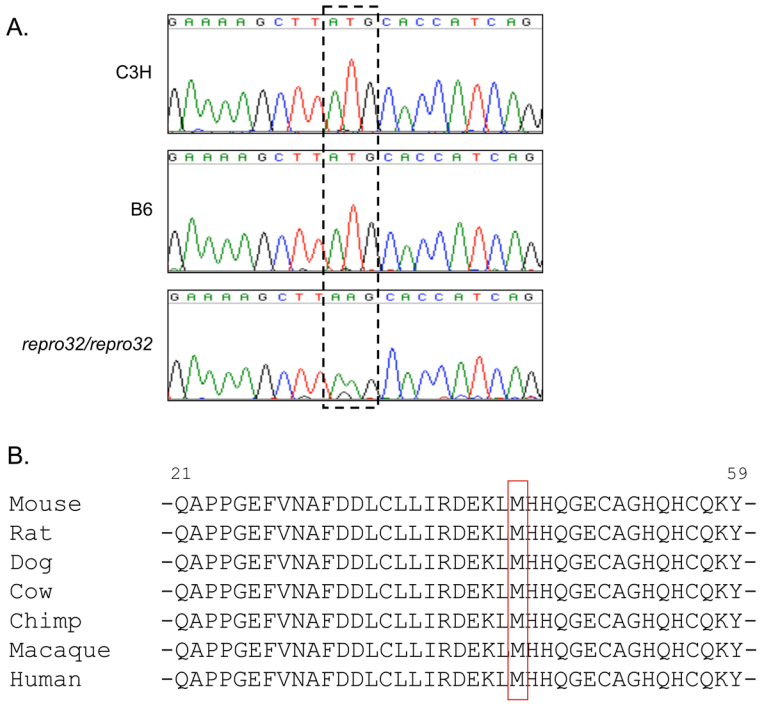

Figure 4.

A missense mutation (M44K) is present in the *Capza3* gene in *repro32*/*repro32* mice. (A) Partial mouse *Capza3* coding sequence (nt 121-141, GenBank sequence NM_007605) from parental strains C3H and B6 and mutant strain *repro32/repro32* mice. A T/A transversion changes an ATG to an AAG codon (dashed box). (B) A region of the CAPZA3 sequence common to the species indicated. The resultant missense mutation replaces a methionine (M, red box) with a lysine at position 44.

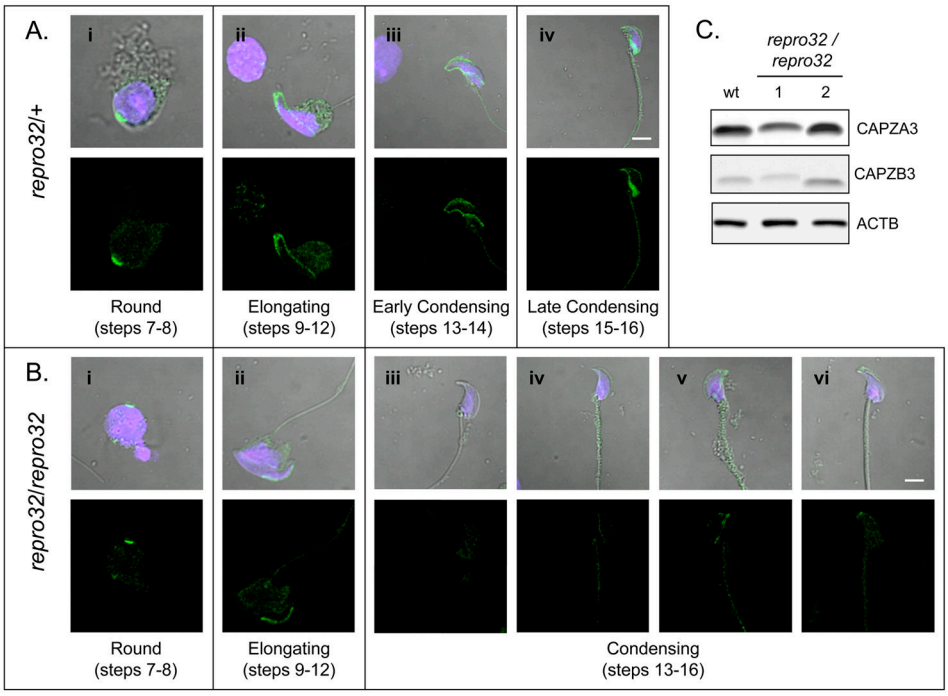

Figure 5.

CAPZA3 localization and levels in spermatids. IIF with antiserum to CAPZA3 (green) on *repro32*/+ round (A.i), elongating (A.ii), early condensing (A.iii), and late condensing (A.iv) spermatids. CAPZA3 localization in *repro32/repro32* round (B.i), elongating (B.ii) and condensing (B.iii–vi) spermatids. Upper panels = merged CAPZA3 IIF (green), DAPI (blue) and DIC images, lower panels = CAPZA3 IIF only. Scale bars = 2μ. (C) Immunoblot of the insoluble fraction of whole testis lysates from wild type and two *repro32/repro32* mice. ACTB = cytoplasmic beta actin (loading control).

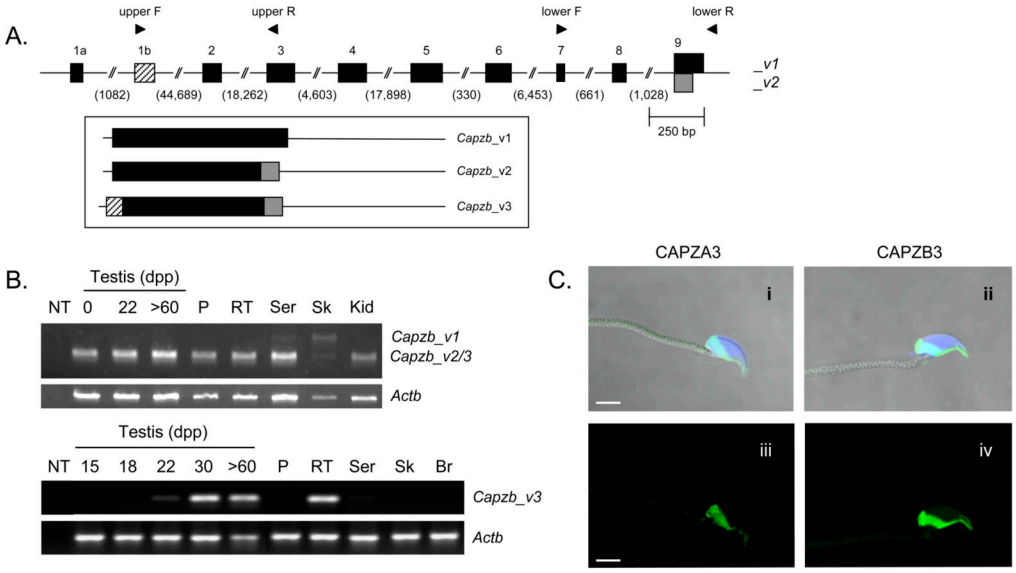

Figure 6.

Genomic organization of a testis-specific *Capzb* transcript variant (*Capzb*_v3) and expression of *Capzb* transcript variants (*Capzb_v1*, *Capzb_v2*, and *Capzb_v3*) in the mouse. (A) The testis-specific *Capzb_v3* transcript contains a unique N-terminal extension resulting from utilization of alternate exon 1b. *Capzb_v1* and *Capzb_v2* utilize exon 1a, but *Capzb_v2* differs from *Capzb_v1* due to alternative splicing that omits 113 nucleotides within exon 9. (B) RT-PCR using *Capzb* variant-specific primers (locations shown in A, upper F/R, lower F/R) to amplify 50 ng of cDNA from various tissues (NT = no template control, 0 ->60 dpp = whole testis aged in days post partum; P = pachytene spermatocytes, RT = round spermatids, Ser = Sertoli cells, Sk = skeletal muscle, Kid = kidney, Br = whole brain). *Actb* = cytoplasmic beta actin. (C) Testicular sperm from *repro32/+* mice; (C.i) merged CAPZA3 IIF (green) and DAPI (blue); (C.iii) CAPZA3 IIF only; (C.ii) merged CAPZB IIF and DAPI; (C.iv) CAPZB3 IIF only. Scale bars = 2μ

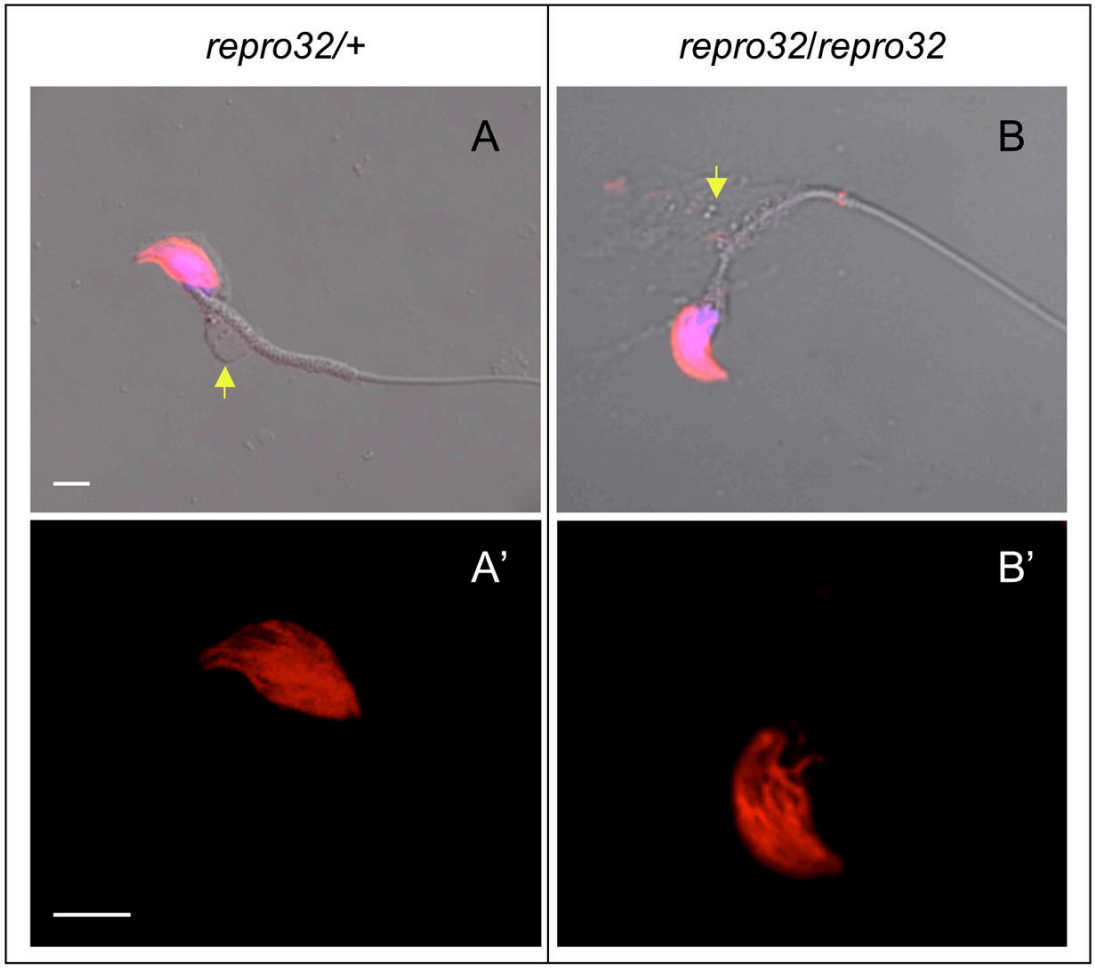

Figure 7.

Mechanically isolated spermatids from *repro32/+* and *repro32/repro32* mice with associated ES-containing Sertoli cell remnants. The F-actin fibers of the ES are labeled with fluorescent dye-conjugated phalloidin (red). (A) *repro32/+* spermatid labeled with phalloidin and DAPI; (A′) enlarged image of same *repro32/+* spermatid labeled with phalloidin alone; (B) *repro32/repro32* spermatid stained with phalloidin and DAPI; (B′) enlarged image of same *repro32/repro32* labeled with phalloidin alone. Cytoplasmic remnants are indicated by yellow arrows. Scale bars = 2μ.

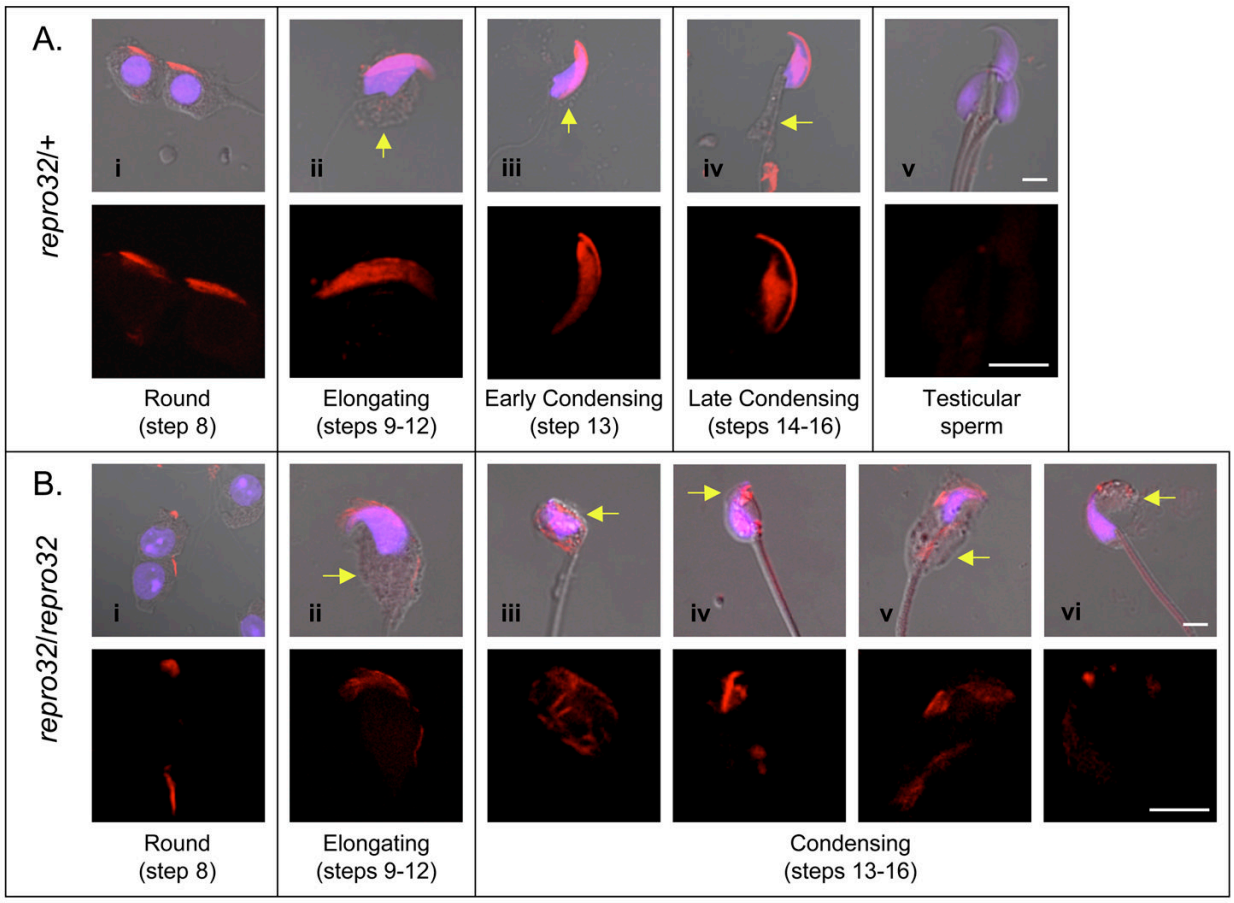

Figure 8.

Sertoli cell ESs have been removed from developing spermatids by trypsin treatment. (A) F-actin labeled with fluorescent dye-conjugated phalloidin (red) in *repro32*/+ (A.i) step 8 round, (A.ii) elongating, (A.iii) early condensing, and (A.iv) late condensing spermatids. F-actin was not detected in testicular sperm (A.v). (B) F-actin fiber development in *repro32/repro32* (B.i) step 8 round, (B.ii) elongating, and (B.iii–vi) condensing spermatids. The upper panels of figures A and B are merged images of DIC, phalloidin-labeled F-actin (red), and DAPI-labeled nuclei (blue), while the bottom panels show phalloidin-labeled F-actin only. Yellow arrows indicate associated cytoplasm. Scale bars = 2μ.

Table 1

Genotype	n	Body weight (g)	Testis weight (g)	Paired seminal vesicle weight (g)	Sperm count (10^6/ml)[b]	Sperm morphology	Sperm motility
repro32/+	9	38.6 ± 3.8	0.110 ± 0.012	0.281 ± 0.047	14.39 ± 2.04	Normal	Motile
repro32/repro32	13	38.0 ± 11.6	0.090 ± 0.020	0.323 ± 0.135	3.54 ± 2.30[c]	Abnormal	Immotile

[a] Values are means ± SEM

[b] The number of sperm collected from one cauda epididymis into 1 ml

[c] Significant difference at P<0.01